THE JOURNAL OF BIOLOGICAL CHEMISTRY
Vol. 280, No. 1, Issue of January 7, pp. 506–514, 2005

Printed in U.S.A.

Controlling the Regiospecific Oxidation of Aromatics via Active Site Engineering of Toluene *para*-Monooxygenase of *Ralstonia pickettii* PKO1*

Received for publication, September 8, 2004, and in revised form, October 18, 2004
Published, JBC Papers in Press, October 21, 2004, DOI 10.1074/jbc.M410320200

Ayelet Fishman, Ying Tao, Lingyun Rui, and Thomas K. Wood‡

From the Departments of Chemical Engineering and Molecular and Cell Biology, University of Connecticut, Storrs, Connecticut 06269-3222

A primary goal of protein engineering is to control catalytic activity. Here we show that through mutagenesis of three active site residues, the catalytic activity of a multicomponent monooxygenase is altered so that it hydroxylates all three positions of toluene as well as both positions of naphthalene. Hence, for the first time, an enzyme has been engineered so that its regiospecific oxidation of a substrate can be controlled. Through the A107G mutation in the α-subunit of toluene *para*-monooxygenase, a variant was formed that hydroxylated toluene primarily at the *ortho*-position while converting naphthalene to 1-naphthol. Conversely, the A107T variant produced >98% *p*-cresol and *p*-nitrophenol from toluene and nitrobenzene, respectively, as well as produced 2-naphthol from naphthalene. The mutation I100S/G103S produced a toluene *para*-monooxygenase variant that formed 75% *m*-cresol from toluene and 100% *m*-nitrophenol from nitrobenzene; thus, for the first time a true *meta*-hydroxylating toluene monooxygenase was created.

Enzymes are attractive catalysts for chemical synthesis because of their exceptional enantio- and regioselectivities; hence, enzymes can be used in both simple and complex syntheses without the need for the blocking and deblocking steps often found in their organic counterparts (1, 2). The number of biocatalytic processes that are being performed on a large scale is rapidly increasing, and it is projected that this growth will continue (3, 4) to become 30% of the chemical business by the year 2050 (5). Although the majority of currently used industrial enzymes are hydrolases (4), there is growing interest in the application of oxygenases (5). Oxidative biotransformations use oxygen as an inexpensive, environmentally friendly oxidant in contrast to toxic chemical oxidants, and they exceed their chemical equivalent in regiospecificity and enantioselectivity (6, 7). Among bacterial oxygenases, toluene monooxygenases have a lot of potential for bioremediation and chemical synthesis, as we have used mutagenesis to make, among other things, variants that remediate one of the world's worst pollutants (trichloroethylene) (8), form a rainbow of colors from indole with a single enzyme, and make the anti-cancer compound indirubin (9). These variants also make useful compounds like 1-naphthol (15,000 ton/year market) (8), nitrohydroquinone (precursor for therapeutics for Alzheimer and Parkinson disease) (10), and 4-nitrocatechol (inhibitor of nitric-oxide synthase) (11). For these industrial applications, control of regiospecific oxidation of aromatics is of vital importance. Further, regiospecific oxidation of toluene, substituted benzenes, and naphthalene by these monooxygenases presents an important challenge both in terms of the three distinct regiospecific oxidations possible for the initial hydroxylation of toluene as well as in terms of the usefulness of both the mono- and dihydroxylated products.

Toluene *para*-monooxygenase (TpMO,[1] formerly known as T3MO) of *Ralstonia pickettii* PKO1 is a soluble, non-heme, diiron monooxygenase (12) and is composed of six proteins encoded by *tbuA1UBVA2C* (13). TbuA1, TbuA2, and TbuU are the α-, β-, and γ-subunits, respectively, of the hydroxylase component (209 kDa with $\alpha_2\beta_2\gamma_2$ quaternary structure), which controls regiospecificity (14, 15). TbuB is a Rieske-type [2Fe-2S] ferredoxin (12.3 kDa), and TbuV is an effector protein (11.7 kDa). TbuC is an NADH oxidoreductase (36.1 kDa) that is responsible for the transfer of electrons from reduced nucleotides via the redox center to the terminal oxygenase (13). *R. pickettii* PKO1 cells expressing the TpMO pathway were shown to degrade trichloroethylene when induced by toluene or trichloroethylene (16, 17).

The original characterization of TpMO as a *meta*-hydroxylating enzyme that is capable of transforming toluene to *m*-cresol (18) was found to be incorrect, as Wood and co-workers (19) have shown that TpMO produces 90% *p*-cresol and 10% *m*-cresol from toluene and successively oxidizes these to 4-methyl catechol. This result is in agreement with the work of Tao *et al.* (20) and Vardar and Wood (21), which shows that the four monooxygenases, TpMO, toluene 4-monooxygenase (T4MO) of *Pseudomonas mendocina* KR1, toluene *ortho*-monooxygenase (TOM) of *Burkholeria cepacia* G4, and toluene *o*-xylene monooxygenase (ToMO) of *Pseudomonas stutzeri* OX1 hydroxylate benzene successively to phenol, catechol, and 1,2,3-trihydroxybenzene.

Fox and co-workers (14, 15, 22) previously found mutations in the related enzyme T4MO of *P. mendocina* KR1 that influence its regiospecificity. From toluene, the α-subunit variant TmoA T201F yielded nearly equal amounts of *o*- and *p*-cresol (49.1 and 46.6%, respectively) and a substantial amount of benzyl alcohol (11.5%) compared with the wild-type enzyme, which makes 97% *p*-cresol and 3% *m*-cresol (14). F205I, an-

* This research was supported by National Science Foundation Grant BES-0124401 and by the United States Environmental Protection Agency. The costs of publication of this article were defrayed in part by the payment of page charges. This article must therefore be hereby marked "*advertisement*" in accordance with 18 U.S.C. Section 1734 solely to indicate this fact.

‡ To whom correspondence should be addressed. Tel.: 860-486-2483; Fax: 860-486-2959; E-mail: twood@engr.uconn.edu.

[1] The abbreviations used are: TpMO, toluene *para*-monooxygenase; T4MO, toluene 4-monooxygenase; TOM, toluene *ortho*-monooxygenase; ToMO, toluene *o*-xylene monooxygenase; MP, methoxyphenol; NP, nitrophenol; MB, methoxybenzene; NB, nitrobenzene; HPLC, high-pressure liquid chromatography; ee, enantiomeric excess.

other beneficial T4MO TmoA mutant, produced 81% *p*-cresol, 14.5% *m*-cresol, and insignificant amounts of *o*-cresol and benzyl alcohol (22). The most notable change was found with mutant TmoA G103L, which influenced the selectivity for *ortho*-hydroxylation of toluene, yielding 55.4% *o*-cresol (15). Tao *et al.* (23) reported the α-subunit positions Gly-103 and Ala-107 of T4MO influenced the rate and regiospecific oxidation of *o*-methoxyphenol (*o*-MP) and *o*-cresol. A double mutant, G103A/A107S, produced 83% 3-methoxycatechol from *o*-MP 7-fold faster than wild-type T4MO, which produced 87% 4-methoxyresorcinol (23). The analogous position to TmoA Ala-107 in TOM of *B. cepacia* G4, TomA3 Ala-113, was also shown to influence the regiospecific oxidation of indigoids (9). For example, variant TomA3 A113V oxidized indole to 89% indigo and variant A113I produced 64% indirubin, whereas the wild-type produces 86% isoindigo. Fishman *et al.* (11) revealed that position TmoA Ile-100 of T4MO is also important for regiospecific oxidation in that variants I100S and I100A produced *m*-nitrophenol from nitrobenzene, whereas the wild-type enzyme produced *p*-nitrophenol. A recent report on the mutagenesis of TOM of *B. cepacia* G4 (24) indicated that the analogous position to T4MO TmoA Ile-100, TomA3 Val-106, changes the regiospecificity of TOM from a conserved *ortho*-hydroxylating enzyme to a nonspecific catalyst, producing all three cresol isomers from toluene.

Recently, the crystal structure of ToMO of *P. stutzeri* OX1 was published, shedding light on the importance of various active site residues on the catalytic activity of this enzyme (25). Currently there are no reports on the mutagenesis of TpMO.

As there is no known enzyme that hydroxylates primarily at the *meta*-position for toluene (19), we were interested in performing mutagenesis on TpMO to enable it to make substantial amounts of *meta*-hydroxylated compounds from substituted benzenes. Furthermore, we also wanted to fine-tune the regiospecificity of TpMO, via saturation or site-directed mutagenesis, to render it an *ortho*-hydroxylating enzyme similar to TOM or a more complete *para*-hydroxylating enzyme than even wild-type T4MO. It was found that positions Ile-100, Gly-103, and Ala-107 in the TbuA1 hydroxylase subunit govern these changes in regiospecificity. This is the first report of the transformation of a single enzyme into a regiospecific catalyst that hydroxylates the aromatic ring at all possible positions, producing *ortho*-, *meta*-, and *para*-cresols from toluene and producing 1- and 2-naphthol from naphthalene. (There are no previous reports of producing 2-naphthol with microorganisms, and the Western world demand for 2-naphthol is 3-fold greater than for 1-naphthol (26).) Evidence of these regiospecific shifts are also shown with nitrobenzene and methoxybenzene. Structure-function relationships of the mutants were probed based on substrate and product docking into the active site of the TpMO variants.

EXPERIMENTAL PROCEDURES

Chemicals—Nitrobenzene (NB) and naphthalene were purchased from Fisher, and *p*-cresol, methoxybenzene (MB), benzyl alcohol, 3-methoxyphenol (*m*-MP), *o*-nitrophenol (*o*-NP), *m*-nitrophenol (*m*-NP), and *p*-nitrophenol (*p*-NP) were obtained from Acros Organics (Morris Plains, NJ). *o*-Cresol, *m*-cresol, 1-naphthol, 2-naphthol, 4-methoxyphenol (*p*-MP), and 2-methoxyphenol (guaiacol, *o*-MP) were obtained from Aldrich. All materials used were of the highest purity available and were used without further purification.

Bacterial Strains and Growth Conditions—Escherichia coli TG1 (27) with the plasmid constructs was routinely cultivated at 37 °C with shaking at 250 rpm on a C25 incubator shaker (New Brunswick Scientific Co., Edison, NJ) in Luria-Bertani medium (27) supplemented with kanamycin at 100 μg/ml to maintain the plasmids. To stably and constitutively express the toluene monooxygenase genes from the same promoter, the expression vectors pBS(Kan)TOM (8), pBS(Kan)TpMO (20), and pBS(Kan)T4MO (20), were constructed as described earlier.

All experiments were conducted by diluting overnight cells to an optical density (OD) at 600 nm of 0.1 to 0.2 and growing to an OD of 1.2. The exponentially grown cells were centrifuged at 13,000 $\times$ *g* for 8 min at 25 °C in a Beckman J2-HS centrifuge and resuspended in Tris-HNO_3 buffer (50 mM, pH 7.0) or potassium phosphate buffer (50 mM, pH 7.0) for performing the desired oxidation reaction. Expression of wild-type TpMO from pBS(Kan)TpMO (henceforth TG1(TpMO)) or T4MO from pBS(Kan)T4MO (henceforth TG1(T4MO)) within *E. coli* strains produced blue-colored cells on agar plates and in broth cultures. The blue color is indicative of indigo, formed by oxidation of indole from tryptophan (28). Expression of wild-type TOM from pBS(Kan)TOM (henceforth TG1(TOM)) within *E. coli* strains produced the normal brown-colored cells on agar plates and in broth cultures (29) as a result of isoindigo formation (9).

Protein Analysis and Plasmid Manipulation—Cellular protein samples of cells grown with and without 1 mM isopropyl β-D-thiogalactopyranoside were analyzed on standard 12% Laemmli discontinuous SDS-polyacrylamide gels (27). The protein content of TG1(TpMO) and TG1(T4MO) was 0.24 mg of protein/(ml·OD) and 0.22 mg of protein/(ml·OD) for TG1(TOM) (20).

DNA Sequencing—A dideoxy chain termination technique (30) with the ABI™ Prism BigDye terminator cycle sequencing ready reaction kit and ABI™ 373 DNA sequencer (PerkinElmer Life Sciences) was used to determine the nucleotide sequence of the TpMO TbuA1 mutants using primer TpMO BamHI Front (see Table I). Plasmids were isolated using a mini or midi kit (Qiagen, Inc., Chatsworth, CA.).

Mutagenesis—Site-directed mutagenesis and saturation mutagenesis were performed as described previously (11, 23, 24). Two PCRs were conducted to randomize or specifically change the desired position at one end of the fragment while introducing a restriction site for cloning at the opposite end. A third PCR reaction using the two initial fragments as templates was performed to obtain the final fragment with the two cloning sites at the ends. The resulting PCR product containing randomized nucleotides at TbuA1 position 100, 103, or 107 was cloned into pBS(Kan)TpMO after double digestion with KpnI and BclI, replacing the corresponding fragment in the original plasmid. The four primers used to obtain mutations in the positions TbuA1 Ile-100, TbuA1 Gly-103, and TbuA1 Ala-107 are shown in Table I.

Screening Method—The screening method used to identify mutants with a different activity than wild-type TpMO was described earlier (11, 23). Briefly, the *E. coli* TG1 transformants were plated on a Luria-Bertani agar plate containing 100 μg/ml kanamycin and 1% w/v glucose. Following overnight incubation at 37 °C, the colonies were transferred to Luria-Bertani plates containing 100 μg/ml kanamycin and 1 mM desired substrate using a nylon membrane. The substrates used in this work were toluene, NB, MB, *o*-cresol, and *o*-MP. Colonies exhibiting halo colors or intensities different from wild-type TpMO on the nylon membranes were further evaluated for their regiospecificity on substituted benzenes.

Enzymatic Activity—Oxidation of NB, MB, and naphthalene was determined using reverse-phase high-pressure liquid chromatography (HPLC). Two milliliters of concentrated cell suspensions (OD of 8) in Tris-HNO_3 buffer (50 mM, pH 7.0) were contacted with substrates at concentrations specified in Table II (from a 100-mM stock solution in ethanol) in 15-ml serum vials sealed with Teflon-coated septa and aluminum crimp seals. The negative controls used in these experiments contained the same monooxygenase without substrates (plus solvent) as well as TG1/pBS(Kan) with substrates (no monooxygenase control). The inverted vials were shaken at room temperature at 300 rpm on an IKA-Vibrax-VXR shaker (Cincinnati, OH) for 2.5–30 min, and then 1 ml of the cell suspension was removed and centrifuged in a 16 M Labnet Spectrafuge (Edison, NJ) for 1–2 min. The supernatant was filtered and analyzed. Toluene oxidation was performed as described earlier (24). Two to three independent experiments were performed to characterize each strain with each substrate described in this paper.

Analytical Methods—Oxidation of NB, MB, and naphthalene was measured using HPLC. Filtered samples were injected into a Zorbax SB-C8 column (Agilent Technologies, 5 μm, 4.6 $\times$ 250 mm) with a Waters Corporation (Milford, MA) 515-solvent delivery system coupled to a photodiode array detector (Waters 996). The gradient elution for detecting NB oxidation products was performed with H_2O (0.1% formic acid) and acetonitrile (70:30 for 0–8 min, gradient to 40:60 at 15 min, and gradient to 70:30 at 20 min) as the mobile phase at a flow rate of 1 ml/min. The gradient elution for detecting MB products was gradient at 80:20 for 0–17 min, gradient to 50:50 at 22 min, and gradient to 80:20 at 30 min. For naphthalene oxidation products, the gradient elution was gradient at 65:35 for 0–5 min, gradient to 35:65 at 12 min, and gradient to 65:35 at 20 min. Compounds were identified by comparing

TABLE I

Primers used for mutagenesis (site-directed mutagenesis of TbuA1 I100S and I100S/G103S and saturation mutagenesis of TbuA1 Gly-103 and Ala-107) and sequencing of the tbuA1 gene in pBS(Kan)TpMO

Restriction enzyme sites indicated in the primer name are underlined. The mutated position is bold and underlined.

Method	Primer	Nucleotide sequence
TbuA1 I100S	TpMO I100S Front	5′-CGCC**AGT**GCGCTCGGCGAATACGCAG-3′
	TpMO I100S Rear	5′-CTCATCGCTGCGTATTCGCCGAGCGC**ACT**GGCG-3′
	TpMO 107 F outer	5′-GACCATGATTACGCCAAGCGCGC-3′
	TpMO AF Rear	5′-GCGCCAGAACCAGATGCCCATC-3′
TbuA1 I100S/G103S	TpMO I100S/G103S Front	5′-GCC**AGT**GCGCTC**AGC**GAATACGCAGCG-3′
	TpMO I100S/G103S Rear	5′-CTCATCGCTGCGTATTC**GCT**GAGCGC**ACT**GGCG-3′
	TpMO 107 F outer	5′-GACCATGATTACGCCAAGCGCGC-3′
	TpMO AF Rear	5′-GCGCCAGAACCAGATGCCCATC-3′
TbuA1 Gly-103	TpMO G103 Front	5′-CACTACGGCGCCATTGCGCTC**NNN**GAATACGCAGCG-3′
	TpMO G103 Rear	5′-CGGCGCTCATCGCTGCGTATTC**NNN**GAGCGCAATG-3′
	TpMO 107 F outer	5′-GACCATGATTACGCCAAGCGCGC-3′
	TpMO AF Rear	5′-GCGCCAGAACCAGATGCCCATC-3′
TbuA1 Ala-107	TpMO A107 Front	5′-CATTGCGCTCGGCGAATACGCA**NNN**ATGAGCGCC-3′
	TpMO A107 Rear	5′-CCATGCGTGCCTCGGCGCTCAT**NNN**TGCGTATTCG-3′
	TpMO 107 F outer	5′-GACCATGATTACGCCAAGCGCGC-3′
	TpMO AF Rear	5′-GCGCCAGAACCAGATGCCCATC-3′
Sequencing	TpMO BamHI Front	5′-TGAGGGATCCCGCCAAGCAAAAAACACTAC-3′

retention times and UV-visible spectra with those of authentic standards as well as by co-elution with standards. Toluene oxidation was measured using gas chromatography analysis as described previously (23, 24).

Substrate Docking and Modeling of TpMO Mutants—The substrate docking simulations were performed using the Lamarckian genetic algorithm (31) of AutoDock version 3.0 (32). Multiple docking runs were performed for each substrate and each variant; the conformations with the overall lowest energies were considered for further analysis. The protein coordinates of the wild-type TpMO α-subunit that was used for the docking simulations were constructed using the experimental structure of the hydroxylase subunit of ToMO of *P. stutzeri* OX1 (25) (Protein Data Bank accession code 1TOQ) via SWISS-MODEL server (33–35). The coordinates of the TpMO variants were built by introducing substitutions in the wild-type TpMO model using Swiss-PdbViewer (33–35), and a single rotamer was selected based on the criterion that the side chain conformation is at the lowest energy state. Polar hydrogen atoms were added to the protein, and charges were assigned to each atom using AutoDockTools. The structures of the ligand molecules toluene, *m*-cresol, and *p*-cresol were obtained from the Protein Data Bank (accession codes 1R1X, 1EV6, and 1JHV, respectively); the structure of *o*-cresol was generated by Chem3D (CambridgeSoft Inc., Cambridge, MA); and energy was minimized by MOPAC using the PM3 Hamiltonian (CAChe Group, Beaverton, OR). Prior to automatic docking using AutoDock, the ligand coordinates were manually modified so they were near the active site center of TpMO α-subunit model.

RESULTS

Saturation and Site-directed Mutagenesis—Two gene libraries encoding all possible amino acids at codons 103 and 107 of TpMO *tbuA1* in pBS(Kan)TpMO (20) were constructed by replacing the target codon with NNN via overlap-extension PCR (24, 36) where N is nucleotide A, G, T, or C. Saturation mutagenesis was chosen because it provides much more comprehensive information than can be achieved by single amino acid substitutions and because it overcomes the disadvantages of random mutagenesis, in that a single mutation randomly placed in codons generates on average only 5.6 of 19 possible substitutions (37).

Codon 103 was chosen for mutagenesis based on previous results with T4MO of *P. mendocina* KR1, which indicate that this position is important for regiospecific oxidation of substituted benzenes (15, 23), and position 107 was selected based on earlier results with T4MO (23) and with the analogous position (TomA3 113) in TOM of *B. cepacia* G4 (9, 23). The screening method developed in our laboratory focused initially on identifying mutants with the ability to form catecholic compounds. At neutral pH, the catechol derivatives formed from oxidation of the substituted benzenes or phenols by the monooxygenase auto-oxidize to quinones and semiquinones, which readily polymerize and form a red or brown color (11, 23). Three hundred colonies from each of the two libraries were screened on toluene, NB, MB, *o*-cresol, and *o*-MP to ensure that there was a 99% probability that all 64 possible codons from a single site random mutagenesis were evaluated (24). HPLC and gas chromatography were used to further characterize the products from TG1 cells expressing TpMO TbuA1 mutants that showed halo colors different from wild-type TG1(TpMO) on the nylon membranes with the substituted aromatics. Variant TpMO TbuA1 I100S was specifically designed based on recent results with T4MO TmoA I100S, which was found through both error-prone PCR and saturation mutagenesis to exhibit higher *meta*-hydroxylation capabilities than wild-type T4MO (20% *m*-cresol formation from toluene *versus* 3% produced by wild-type T4MO) (11).

The classification of each mutant as an *ortho*-, *meta*-, or *para*-hydroxylating enzyme was based on the identity of the major cresol isomer formed from toluene oxidation. To further characterize each mutant, the product distribution from transformation of NB, MB, and naphthalene was determined. The chemical structures of the various compounds discussed in this work are presented in Fig. 1.

Changing TpMO into an ortho-Hydroxylating Enzyme—Mutant TpMO TbuA1 A107G showed a red halo on an NB plate (indicative of nitrocatechol formation) and was found to produce 80% *o*-cresol from toluene, whereas wild-type TpMO made only negligible amounts of *o*-cresol (Table II, Fig. 2). Oxidation of MB by A107G yielded 88% *o*-MP, whereas wild-type TpMO did not produce this isomer. Variant A107G exhibited similar regiospecificity to TOM of *B. cepacia* G4 for both substrates, although wild-type TOM was more stringent in its *ortho*-hydroxylation capability. In addition, TpMO TbuA1 A107G produced 97% 1-naphthol from naphthalene, whereas wild type TpMO produced 63%, again correlating well with wild-type TOM. Both wild-type TOM and A107G did not hydroxylate NB to *o*-NP as might be expected, and wild-type TOM was totally inactive on this substrate. A107G produced primarily *m*-NP from NB, and the rate of *m*-NP formation by A107G was 6-fold higher than that of wild-type TpMO (0.08 ± 0.04 nmol/min/mg protein *versus* 0.013 ± 0.004, respectively).

Changing TpMO into a Complete para-Hydroxylating Enzyme—T4MO of *P. mendocina* KR1 is a highly regiospecific enzyme, hydroxylating nearly all monosubstituted benzenes tested including toluene, chlorobenzene, MB, and NB at the *para*-position (11, 15). Although wild-type TpMO is a less specific *para*-hydroxylating enzyme (Table II), mutant TpMO

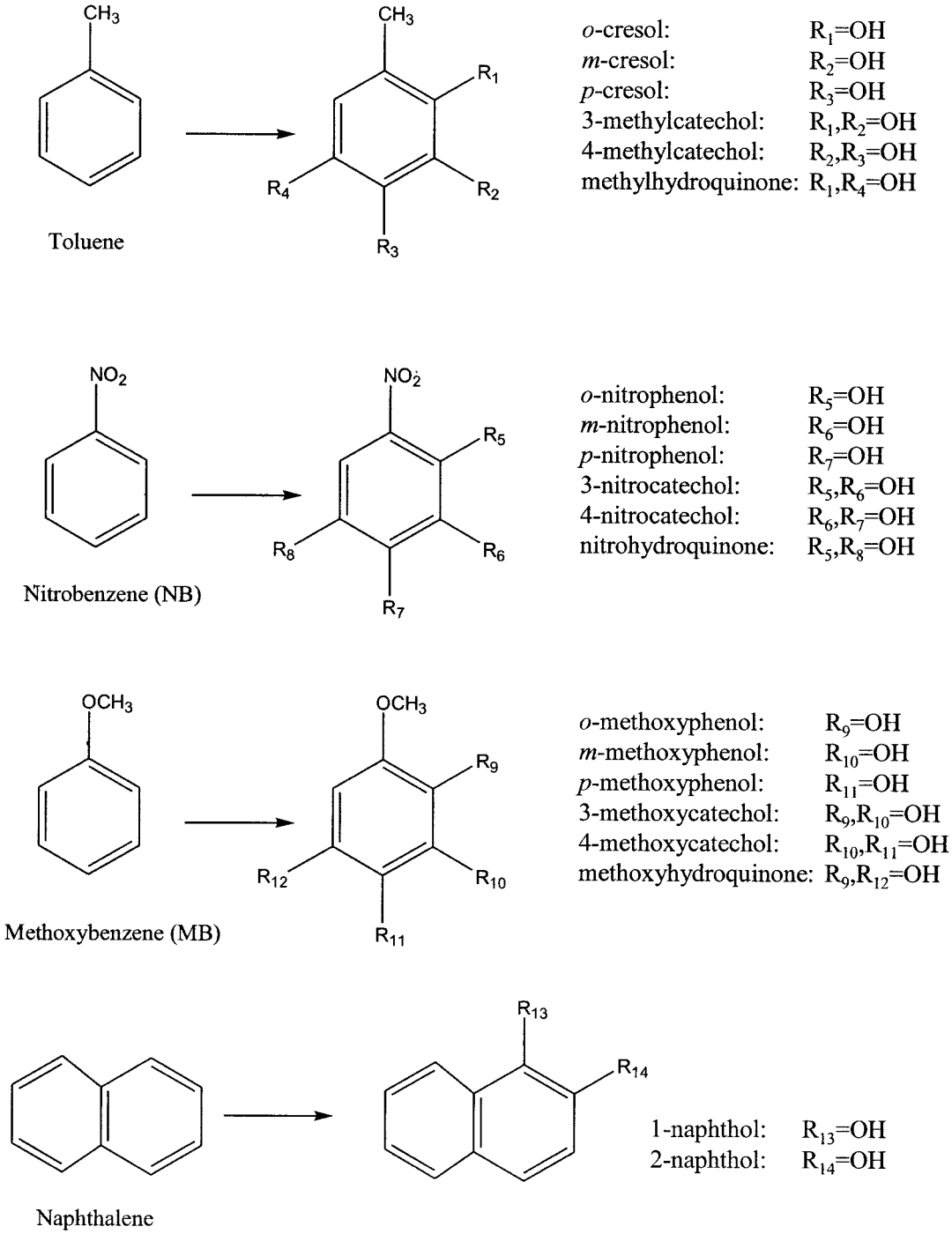

FIG. 1. **Structures of compounds discussed in this study.**

TbuA1 A107T was found to exceed even T4MO in its *para*-specificity (Table II, Fig. 2). TbuA1 A107T hydroxylated toluene, NB, and MB to their corresponding *para*-substituted phenols at specificities of >98%. In comparison, T4MO produced 97% *p*-cresol from toluene and only 90% *p*-NP from NB. A107T also produced significant amounts of 2-naphthol compared with wild-type TpMO.

Changing TpMO into a meta-Hydroxylating Enzyme—Previous work with mutants of T4MO of *P. mendocina* KR1 revealed that variant T4MO TmoA I100S is a more relaxed enzyme in terms of regiospecificity, capable of forming 20% *m*-cresol from toluene (11). Variant TbuA1 I100S, the analogous TpMO mutant constructed here, formed 33% *m*-cresol (compared with the 10% produced by wild-type TpMO) and 65% *m*-NP from NB (Table II). This variant was a better catalyst than wild type in terms of activity, exhibiting a higher toluene oxidation rate by 68% and a 10-fold greater rate for *m*-NP formation (0.145 ± 0.016 nmol/min/mg protein *versus* 0.013 ± 0.004).

Another *meta*-hydroxylating enzyme was found by screening the two mutant libraries on *o*-cresol. Enzyme TbuA1 G103S formed 29% *m*-cresol from toluene and 96% *m*-NP from NB (Table II). This result corroborated well with T4MO TmoA G103S, which produced 17% *m*-cresol from toluene compared with 3% produced by wild-type T4MO (23). The *m*-NP formation rate by TbuA1 variant G103S was very high (100-fold activation; 1.25 ± 0.064 nmol/min/mg protein *versus* 0.013 ± 0.004 for wild-type), leading to the high regiospecificity observed for this substrate.

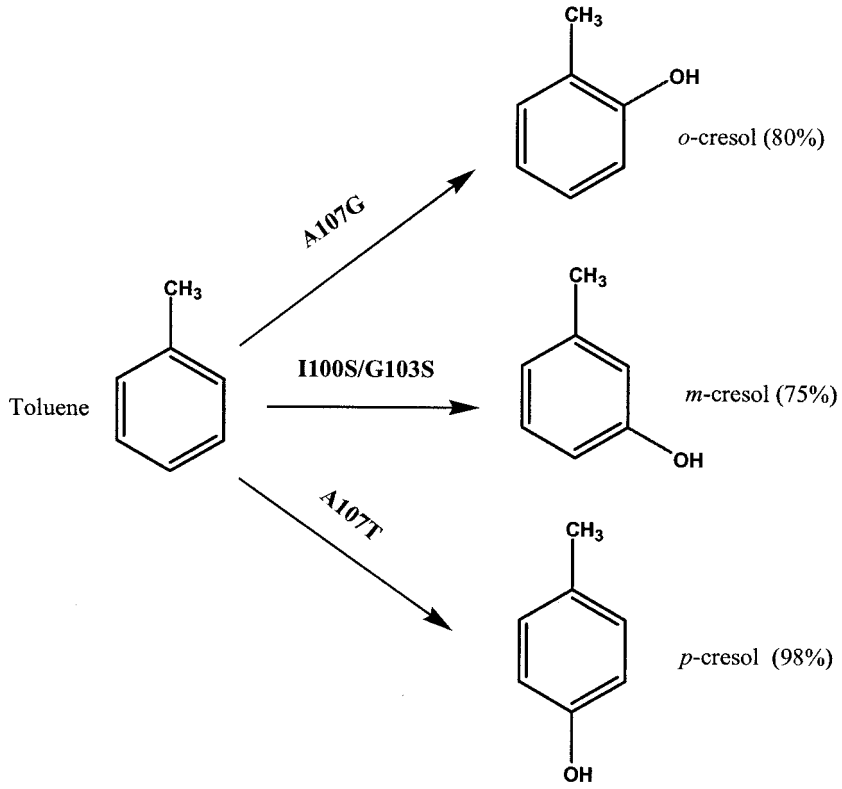

FIG. 2. **Regiospecificity of toluene oxidation by the TpMO TbuA1 mutants A107G (*o*-cresol), I100S/G103S (*m*-cresol), and A107T (*p*-cresol).** Note that wild-type TpMO produces 88% *p*-cresol, 10% *m*-cresol, and 2% *o*-cresol.

TABLE II

Regiospecific oxidation of toluene (with rate), NB, MB, and naphthalene by TG1 cells expressing wild-type (WT) TOM, WT T4MO, WT TpMO, and TpMO TbuA1 mutants

Each experiment with an enzyme and substrate was conducted twice with independent cultures, and the results represent an average of these data (determined with two to three time points).

Enzyme	Toluene rate[b]	Toluene oxidation[a,b]			NB oxidation[c]			MB oxidation[d]			Naphthalene oxidation[e]	
		o-cresol	*m*-cresol	*p*-cresol	*o*-NP	*m*-NP	*p*-NP	*o*-MP	*m*-MP	*p*-MP	1-Naphthol	2-Naphthol
	nmol/min·mg protein											
WT TOM	1.30 ± 0.06	100	0	0	0	0	0	100	0	0	100	0
WT T4MO	4.40 ± 0.3	1	2	97	0	10	90	0	0	100	52	48
WT TpMO	2.20 ± 0.2	2	10	88	0	34	66	0	0	100	63	37
TbuA1 I100S	3.70 ± 0.7	0	33	67	0	65	35	0	0	100	17	83
TbuA1 G103S	0.74 ± 0.06	8	29	63	0	96	4	28	4	68	80	20
TbuA1 I100S/G103S	1.43 ± 0.08	0	75	25	0	100	0	0	18	82	43	57
TbuA1 A107G	0.84 ± 0.06	80	6	14	0	85	15	88	0	12	97	3
TbuA1 A107T	0.62 ± 0.1	0	2	98	0	0	100	0	0	100	27	73

[a] Initial rate of toluene oxidation from a linear plot of substrate degradation with time (liquid phase concentration 90 μM based on Henry's law constant of 0.27 (56); 250 μM added if all the toluene in the liquid phase).

[b] Benzyl alcohol was formed in negligible amounts by WT T4MO and TpMO with <1.5%.

[c] Based on HPLC analysis over a 45 min time period (initial NB concentration was 200 μM).

[d] Based on HPLC analysis over a 60 min time period (initial MB concentration was 500 μM).

[e] Based on HPLC analysis over a 2 h time period (initial naphthalene concentration was 5 mM). Naphthalene solubility in water is 0.23 mM (47).

To enhance the *meta*-hydroxylating capabilities of TpMO, the double mutant TbuA1 I100S/G103S was generated. This mutant produced 75% *m*-cresol and 25% *p*-cresol from toluene (Table II, Fig. 2) and 100% *m*-NP from NB, thus demonstrating predominant *meta*-hydroxylation for the first time.

Toluene Oxidation Rates and Protein Expression Level—The initial toluene oxidation rate was determined for the various TpMO TbuA1 mutants to show that these are active enzymes. I100S had 68% higher activity than wild-type TpMO, but the other mutants had lower activity, with A107T displaying 30% of the wild-type activity.

To verify that the changes in activity and regiospecificity of the TbuA1 mutants derive from the amino acid substitutions rather than expression level changes, SDS-PAGE was used to visualize three of the six subunits: TbuA1 (57.6 kDa), a combined band from TbuA2 (37.5 kDa) and TbuC (36.1 kDa), and a combined band from TbuB (12.3 kDa) and TbuV (11.7 kDa). Mutant and wild-type bands had comparable intensities. In a similar approach, Arnold and co-workers (36) characterized the evolution of toluene dioxygenase using a whole-cell assay and found dramatically increased expression of the (smaller) β-subunit. Furthermore, the ribosome-binding site of the *tbuA1* gene in the TbuA1 variants was unaltered during the mutagenesis as confirmed by DNA sequencing. As the cell growth and the biotransformation conditions were identical for the wild-type and mutants, the changes in activity arise from the mutations at TbuA1 Ile-100, Gly-103, and Ala-107 and not from different expression levels.

Active Site Modeling of TbuA1—To gain insight into the role of active site residues Ile-100, Gly-103, and Ala-107 in controlling the regiospecific oxidation of toluene, a three-dimensional model was constructed based on the known crystal structure of

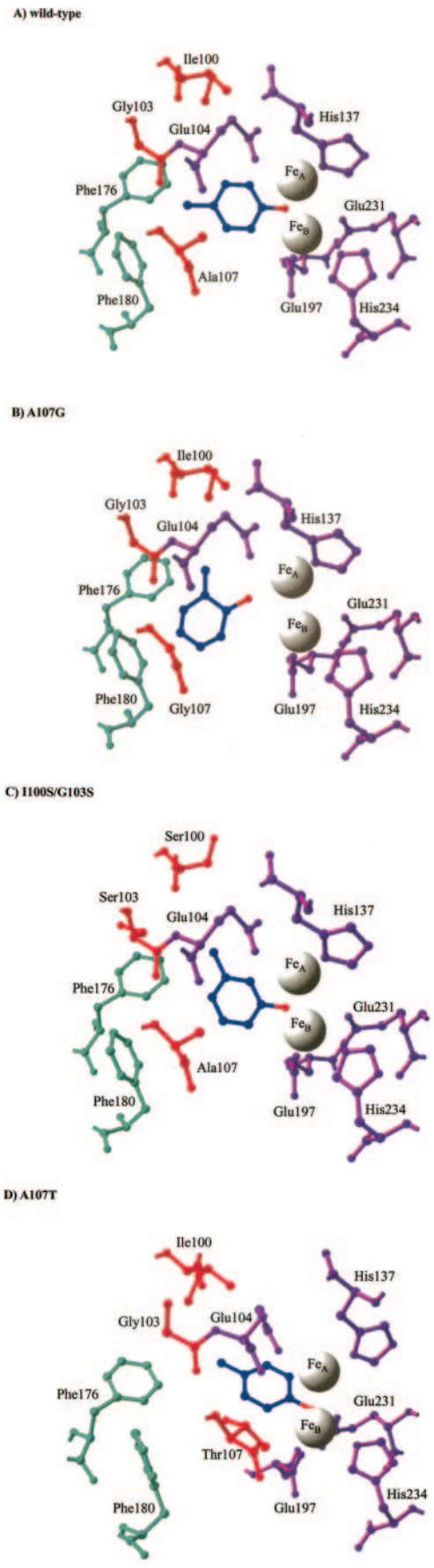

FIG. 3. **Active site of the TbuA1 α-subunit showing mutated residues in *red* at positions Ile-100, Gly-103, and Ala-107.** *A*, wild-type TpMO forming *p*-cresol; *B*, variant A107G forming *o*-cresol; *C*, variant I100S/G103S forming *m*-cresol; and *D*, variant A107T forming *p*-cresol. Residues in *purple* (Glu-104, His-137, Glu-197, Glu-231, and His-234; Glu-134 not shown for clarity) are the coordinating residues anchoring the diiron-binding sites (*silver spheres*). Residues in *light green* are part of the hydrophobic shell (Phe-176 and Phe-180). Cresol (*dark blue* with oxygen in *red*) is docked inside the active site, taking into consideration both energy minimization and steric hindrance.

hydroxylase of ToMO (25) (Fig. 3*A*). The α-subunits TbuA1 of TpMO and TmoA of T4MO share a 68% identity (protein level) with TouA of ToMO (38) and >90% identity in the active site pocket; the main differences are at positions 103 and 180 (25). Both T4MO and TpMO are highly *para*-directing enzymes, indicating that the active site must favor orienting the C-4 position of toluene toward the diiron center (coordinated by TbuA1 residues Glu-104, Glu-134, His-137, Glu-197, Glu-231, and His-234).

To explore the effects of the mutations on regiospecificity, cresols were docked into the active site of the wild-type and altered TbuA1 enzymes. Docking calculations showed significant binding preferences for the favored isoform of each mutant, which coincided well with the experimental data concerning toluene oxidation regiospecificity. For variant A107G, the major change in the active site is the reduced size of the side chain of residue 107, which allows the benzene ring of toluene to shift toward Gly-107 and replace the methyl group of Ala-107, thereby promoting *o*-cresol formation by oxidation of the C-2 (Fig. 3*B*). The same considerations apply for 1-naphthol formation from naphthalene.

The I100S/G103S double mutant that produces 75% *m*-cresol from toluene and 100% *m*-NP from NB may be explained by the increased size of the TpMO channel leading to the Fe_A site (on the side of the active site pocket); this larger space accommodates the methyl group of toluene such that the C-3 is directed toward the diiron center (Fig. 3*C*). Additionally, the presence of serine at position 103 bears a resemblance to glutamic acid at this position in TouA of ToMO (Fig. 4). ToMO produces 21% *m*-cresol from toluene as well as 47% *p*-cresol and 32% *o*-cresol (21), and this lack of specificity is attributed partially to Glu-103 (25). Similar considerations may apply to the *meta*-hydroxylation capability of TbuA1 I100S/G103S.

The A107T mutation appears to restrict the substrates into more rigid positions relative to the diiron center by shrinking the active site (Fig. 3*D*) and may be responsible for the most specific product profile obtained (98% *p*-cresol/2% *m*-cresol and 100% *p*-NP). The hydroxyl group of Thr-107 may form a hydrogen bond with the backbone carbonyl of Gly-103 supporting the orientation of this residue in a way that directs the C-4 in toluene toward the diiron center (forming only *p*-cresol) or the C-2 in naphthalene, resulting in 2-naphthol formation.

DISCUSSION

Toluene monooxygenases have been the subject of many studies in the past few years because of their bioremediation capabilities as well as their potential as biocatalysts for green chemistry (8, 16, 39, 40). Much effort has been placed on understanding the mechanisms by which these complex enzymes work and on the role of various active site residues in activity and selectivity. Most of this work has focused on T4MO of *P. mendocina* KR1 (11, 14, 15, 41), on TOM of *B. cepacia* G4 (8, 24), and on ToMO of *P. stutzeri* OX1 (21, 25). In contrast, TpMO has been studied thoroughly in regard to genetic regulation of the toluene degradation pathway (13, 42–44), but there have been no reports regarding the structure-function relationships for this enzyme. This study aims at filling this gap while expanding the understanding of the correlation between active site residues and regiospecificity of toluene monooxygenases in general.

Positions 100, 103, and 107 of the α-subunit of the hydroxylase protein have been shown here to govern the regiospecificity of TpMO. These residues are located in the active site pocket of the B-helix close to the diiron center (Fig. 3). The residues are four amino acids apart from one another and are spatially located one above the other on the α-helix (45). All three amino acids are part of the hydrophobic region surrounding the active site, which is similar to corresponding residues in other diiron monooxygenases (Fig. 4) (12, 14).

Position TbuA1 Ile-100—Leucine 110 of MmoX in soluble methane monooxygenase of *Methylococcus capsulatus* (Bath), the analogous position to TpMO TbuA1 Ile-100, was shown to divide the active site pocket into two cavities and was hypothesized to function in controlling the access of substrates to the diiron center (46). Support for this role was provided by Canada *et al.* (8) in the first DNA shuffling of a non-heme monooxygenase in which the function of the analogous position in TmoA3 of TOM of *B. cepacia* G4, Val-106, was discerned; the V106A variant hydroxylated bulky three-ring polyaromatics, such as phenanthrene, at higher rates, indicating that a decrease in the size of the side chain allows larger substrates to enter the active site. This variant and two other mutants, V106E and V106F, had decreased regiospecificity for toluene oxidation, altering the strict *ortho*-hydroxylation capability of wild-type TOM to create relaxed catalysts that produce all three cresols (24). In a recent study with T4MO of *P. mendocina* KR1, TmoA mutants I100S and I100A exhibited higher oxidation rates (evidenced by higher apparent V_{max}/K_m values) for toluene, NB, and NP oxidation in comparison with the wild-type enzyme (11). The regiospecificity of toluene and NB oxidation also changed, resulting in higher percentages of the *meta*-isomers. A different TmoA mutant, I100C, had altered enantioselectivity for butadiene epoxidation and formed 60% (*R*)-butadiene epoxide and 40% (*S*)-butadiene epoxide, whereas wild-type T4MO produced 33% (*R*)- and 67% (*S*)-epoxide; however, I100C has a lower toluene oxidation rate.[2] Position Ile-100 in TouA of ToMO of *P. stutzeri* OX1, a nonspecific toluene-oxidizing enzyme, was shown to influence the regiospecific oxidation of cresols and phenol to double hydroxylated products (21). For example, variant I100Q, which was found through saturation mutagenesis, produced 80% hydroquinone and 20% catechol from phenol compared with 100% catechol formed by wild-type ToMO. In addition, this mutant produced substantial amounts of nitrohydroquinone from *m*-NP, whereas wild-type ToMO produced only 4-nitrocathechol (10).

The results with TpMO presented here are in accord with previously reported data on this position. TbuA1 I100S is a highly active enzyme, but its lower regiospecificity enables it to produce higher amounts of *meta*-substituted phenols, similar to TmoA I100S of T4MO (11). The reduced size of the side chain of residue 100 from isoleucine to serine enables the substrate to orient in different configurations in the active site, thus leading to different products. It is also evident that this position, which is originally hydrophobic in nature in all monooxygenases sequenced to date, can tolerate hydrophilic residues as well.

Position TbuA1 Gly-103—The analogous position to TbuA1 Gly-103 has been shown previously to influence both regiospecificity and enantioselectivity. It is adjacent to the glutamic acid residue (TbuA1 Glu-104) that is one of the six conserved iron-binding ligands (Figs. 3 and 4) and is therefore the closest to the active site. A site directed mutant, T4MO TmoA G103L, was designed by Mitchell *et al.* (15) based on other toluene and phenol monooxygenases and was shown to favor *ortho*-hydroxylation more than wild-type T4MO (55.4% *o*-cresol from toluene and 21.6% *o*-MP from MB) except for NB, which was oxidized to 96.4% *m*-NP (15). The TpMO TbuA1 G103S mutant, found here through saturation mutagenesis and screening on *o*-cresol, exhibited similar regiospecificity distribution for NB and MB oxidation but favored *m*-cresol formation from toluene (29%). It seems that the substitution of serine (a hydrophilic residue) for glycine causes alignment of toluene in the active site that is different from that caused by the leucine residue. Position 103 may include a hydrophilic residue in natural monooxygenases, as is evident from ToMO TouA (Fig. 4). This residue was also found to affect the enantioselectivity of propene and butadiene epoxidation. T4MO TmoA G103L produced 90% (*S*)-butadiene epoxide, whereas 67% was produced by wild-type T4MO.[2] The increasing bulkiness of this residue going from methane monooxygenase MmoX (Gly-113) to alkene monooxygenases AmoC from *Rhodococcus rhodochrous* B-276 (Ala-93) and XamoA of *Xanthobacter* Py2 (Val-103), was consistent with their increasing stereospecificity in propene oxidation (48). Recently, the analogous mutant from T4MO, TmoA G103S, was found to change the regiospecificity of *o*-MP oxidation, producing primarily methoxyhydroquinone (80%), whereas wild-type T4MO forms 87% 4-methoxyresorcinol (23).

Position TbuA1 Ala-107—Among the positions discussed in this paper, TbuA1 Ala-107 is conserved in all monooxygenases studied, suggesting that it offers some evolutionary advantage (Fig. 4) (12). Work in our laboratory with TOM of *B. cepacia* G4 showed that this position (TomA3 Ala-113) is involved in color formation of indigoid compounds by influencing whether the two positions of the pyrrole ring or benzene ring are hydroxylated (9). More specifically, variant A113G (analogous to TpMO TbuA1 A107G, found in this work as an *ortho*-hydroxylating enzyme) was found to hydroxylate the indole benzene ring rather than the pyrrole ring oxidized by wild-type TOM. Other variants at this position (A113F, A113S, and A113I) were found to produce high amounts of indirubin from indole oxidation (C-2 and C-3 pyrrole hydroxylation), whereas wild-type TOM produced primarily isoindigo (C-2 pyrrole hydroxylation). TmoA A107S, a T4MO site-directed mutant, was shown to improve the enantioselectivity of butadiene epoxidation,[2] further demonstrating that a hydrophilic residue is tolerable at this conserved position. The two Ala-107 mutants found in this work, TbuA1 A107G (screened from NB plates) and A107T (screened from *o*-cresol plates), had profoundly different hydroxylation regiospecificities. A107G changed the selectivity toward *ortho*-hydroxylation of all three substituted benzenes tested, and A107T improved the *para*-hydroxylating capabilities to exceed even that of the naturally occurring T4MO of *P. medoncina* KR1.

Influence of Substrate on Specificity—The fact that the same enzyme can react differently with several substrates of similar structure (Table II) emphasizes the importance of electrophilic resonance and inductive effects. For example, none of the enzymes formed *o*-NP from NB including the newly constructed *ortho*-hydroxylating TpMO variant TbuA1 A107G and the *ortho*-hydoxylating wild-type TOM. Data reported in Table II corroborate the lack of activity reported previously by Haigler and Spain (49) for the original TOM-harboring strain *B. cepacia* G4. NB is 10 million-fold less reactive than benzene (50), and this may explain the lack of reactivity of TOM toward this substrate. In addition, the nitro group has a strong electron withdrawing ability through inductive and resonance effects, thereby directing the electrophilic substitution to the *meta*-position (50).

The proposed mechanism for aromatic hydroxylation by T4MO (41) involves movement of the aromatic ring with C-4

[2] R. J. Steffan and K. R. McClay, Envirogen Inc., international patent application (WO 2000073425).

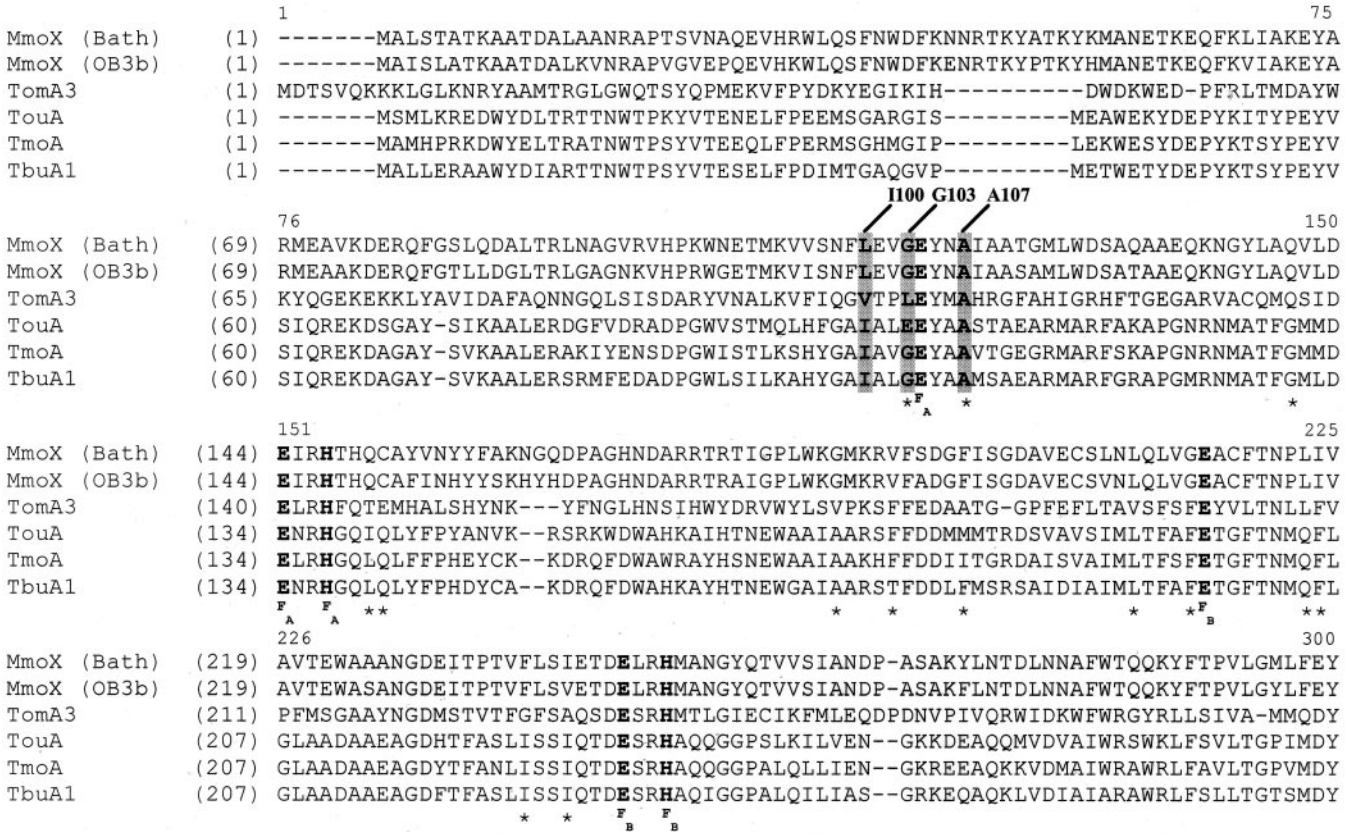

FIG. 4. **Sequence alignments of the amino terminus region of the α-subunits of six soluble diiron monooxygenases.** The amino acid residues analogous to TpMO TbuA1 Ile-100, Gly-103, and Ala-107 are labeled and highlighted in *light gray*. The six residues anchoring the diiron-binding sites are *bold* and labeled by the corresponding diiron atom. Residues comprising the hydrophobic cavity within the active site are marked with an *asterisk*. Sequences were obtained from GenBank™ with the following accession numbers: MmoX from *M. capsulatus* (Bath) (M90050), MmoX (OB3b) from *Methylosinus trichosporium* OB3b (X55394), TomA3 of *B. cepacia* G4 (AF349675), TouA of *P. stutzeri* OX1 (AJ005663), TmoA of *P. mendocina* KR1 (AY552601), and TbuA1 of *R. pickettii* PKO1 (AY541701).

and C-3 approaching the diiron site first, allowing formation of predominantly *p*-substituted phenols. The similarity in structure and function of TpMO and T4MO is high (13) (68% amino acid identity for the α-subunits), and it can be assumed that this mechanism applies for TpMO as well. The product distribution of NB oxidation by wild-type T4MO, wild-type TpMO, and its TbuA1 variants, in which the percentage of *m*-NP formed from nitrobenzene is higher than *m*-cresol formed from toluene, implies again that both active site orientation of the substrate and electronic effects influence the regiospecificity of the reaction. In contrast to NB, the methyl substituent of toluene and the methoxy substituent of MB are *ortho*- and *para*-directing activators, with the methoxy group having more pronounced activation because of the resonance effect (50). Consequently, *para*-hydroxylation is more complete in MB oxidation compared with toluene oxidation (*e.g.* wild-type T4MO, TpMO, TbuA1 I100S, and TbuA1 A107T in Table II).

Novel meta-Hydroxylating Monooxygenase TpMO TbuA1 I100S/G103S—Among the toluene monooxygenases discovered to date, all were reported to perform primarily *ortho*- or *para*-hydroxylation of toluene. Electrophilic considerations may be one explanation for the lack of a primarily *m*-cresol-forming toluene monooxygenase. In addition, the double serine mutant at positions 100 and 103 found here may not be naturally favorable in terms of α-helix stabilization. Different side chains have weak but definite preferences either for or against α-helices. Alanine, glutamic acid, leucine, and methionine are good α-helix formers, whereas proline, glycine, tyrosine, and serine are very poor (45). Consequently, having two serine residues at positions 100 and 103 is not likely because of the hydrophilic nature of serine (in a region of hydrophobic conserved residues), along with the fact that it is not a good α-helix former.

Active Site Modeling—The recent report of the crystal structure of the hydroxylase component of ToMO (25) enabled visualization of the active site of the closely related TpMO. The major limitation of the model arises from the fact that the hydroxylase was crystallized without the effector protein (ToMOD in ToMO and TbuD in TpMO). It has been shown previously for soluble methane monooxygenase that the binding of the effector protein to the hydroxylase induces changes on the active site (51) and alters the regiospecificity of hydroxylation of nitrobenzene (52). In addition, Fox and co-workers (15) have shown that binding of the effector protein of T4MO (T4moD) in variant TmoA T201G conserved the *para*-hydroxylation preference, whereas the same mutant produced mainly *o*-cresol from toluene without the presence of T4moD. Another limitation in the modeling is the docking of the substrate and products rather than the transition state intermediates. Consequently, the exact structure of the active site of TpMO and its TbuA1 mutants may be somewhat different from the ones presented in Fig. 3. Despite these limitations and unknown factors, the model does suggest an explanation for some of the dramatic changes seen in the regiospecificity of the mutants.

Evolving Enzymes for Altered Specificities—Directed evolution is a viable method for altering the enantioselectivity of enzymes. For example, Reetz *et al.* (53) evolved a nonspecific lipase of *Pseudomonas aeruginosa* into a stereoselective enzyme. Wild-type lipase only slightly favored the *S*-ester (2% enantiomeric excess (ee)) in the hydrolysis reaction of 2-methyldecanoic acid *p*-nitrophenyl ester, whereas the error-prone

PCR-derived mutant exhibited an ee of 81%. Subsequent saturation mutagenesis at the "hot spots" increased the selectivity to ee values of 90–94% (54). Using a similar approach, Arnold and co-workers (55) found that a single amino acid substitution (I95F) was sufficient to invert the enantioselectivity of a hydantoinase from D selectivity (40% ee) to moderate L preference (20% ee). A single amino acid substitution (V154A) also greatly improved the moderate D selectivity of the wild type from 40 to 90% ee.

To our knowledge, there have been no analogous complete reports concerning respective changes in regiospecificity. Using saturation and site-specific mutagenesis, we have constructed variants of TpMO with all possible regiospecificities for ring hydroxylation of toluene and naphthalene. By controlling the regiospecificity of the monooxygenase reaction, and given that it may be used to perform as many as three successive hydroxylations (20), a wide range of substituted aromatic products may now be synthesized with these versatile catalysts, including 2-naphthol, as shown here. Furthermore, the structure-function lessons learned here from mutagenesis of TpMO should be directly applicable to the intractable soluble methane monooxygenase of *M. trichosporium* OB3b. Active methane monooxygenase has been expressed only in *Agrobacterium tumefaciens*, *Rhizobium meliloti*, and pseudomonads by our group but never in *E. coli* (57, 58); hence, there are no reports of beneficial mutagenesis of the hydroxylase of this enzyme, the best enzyme for oxidizing methane to methanol.

REFERENCES

1. Schmid, A., Dordick, J. S., Hauer, B., Kiener, A., Wubbolts, M., and Witholt, B. (2001) *Nature* **409,** 258–268
2. Schoemaker, H. E., Mink, D., and Wubbolts, M. G. (2003) *Science* **299,** 1694–1697
3. Straathof, A. J. J., Panke, S., and Schmid, A. (2002) *Curr. Opin. Biotechnol.* **13,** 548–556
4. Kirk, O., Borchert, T. V., and Fuglsang, C. C. (2002) *Curr. Opin. Biotechnol.* **13,** 345–351
5. van Beilen, J. B., Duetz, W. A., Schmid, A., and Witholt, B. (2003) *Trends Biotechnol.* **21,** 170–177
6. Li, Z., van Beilen, J. B., Duetz, W. A., Schmid, A., de Raadt, A., Griengl, H., and Witholt, B. (2002) *Curr. Opin. Chem. Biol.* **6,** 136–144
7. Burton, S. G. (2003) *Trends Biotechnol.* **21,** 543–549
8. Canada, K. A., Iwashita, S., Shim, H., and Wood, T. K. (2002) *J. Bacteriol.* **184,** 344–349
9. Rui, L., Reardon, K. F., and Wood, T. K. (2005) *Appl. Microbiol. Biotechnol.*, **66,** 422–429
10. Vardar, G., Ryu, K., and Wood, T. K. (2005) *J. Biotechnol.*, **115,** 145–146
11. Fishman, A., Tao, Y., Bentley, W. E., and Wood, T. K. (2004) *Biotechnol. Bioeng.* **87,** 779–790
12. Leahy, J. G., Batchelor, P. J., and Morcomb, S. M. (2003) *FEMS Microbiol. Rev.* **27,** 449–479
13. Byrne, A. M., Kukor, J. J., and Olsen, R. H. (1995) *Gene* (*Amst.*) **154,** 65–70
14. Pikus, J. D., Mitchell, K. H., Studts, J. M., McClay, K., Steffan, R. J., and Fox, B. G. (2000) *Biochemistry* **39,** 791–799
15. Mitchell, K. H., Studts, J. M., and Fox, B. G. (2002) *Biochemistry* **41,** 3176–3188
16. Park, J., Kukor, J. J., and Abriola, L. M. (2002) *Appl. Environ. Microbiol.* **68,** 5231–5240
17. Leahy, J. G., Byrne, A. M., and Olsen, R. H. (1996) *Appl. Environ. Microbiol.* **62,** 825–833
18. Olsen, R. H., Kukor, J. J., and Kaphammer, B. (1994) *J. Bacteriol.* **176,** 3749–3756
19. Fishman, A., Tao, Y., and Wood, T. K. (2004) *J. Bacteriol.* **186,** 3117–3123
20. Tao, Y., Fishman, A., Bentley, W. E., and Wood, T. K. (2004) *Appl. Environ. Microbiol.* **70,** 3814–3820
21. Vardar, G., and Wood, T. K. (2004) *Appl. Environ. Microbiol.* **70,** 3253–3262
22. Pikus, J. D., Studts, J. M., McClay, K., Steffan, R. J., and Fox, B. G. (1997) *Biochemistry* **36,** 9283–9289
23. Tao, Y., Fishman, A., Bentley, W. E., and Wood, T. K. (2004) *J. Bacteriol.* **186,** 4705–4713
24. Rui, L., Kwon, Y., Fishman, A., Reardon, K. F., and Wood, T. K. (2004) *Appl. Environ. Microbiol.* **70,** 3246–3252
25. Sazinsky, M. H., Bard, J., Di Donato, A., and Lippard, S. J. (2004) *J. Biol. Chem.* **279,** 30600–30610
26. Howe-Grant, M. (ed) (1991) *Kirk-Othmer Encyclopedia of Chemical Technology*, 4th Ed., Vol. 16, pp. 994–1017, Wiley-Interscience Publishers, New York
27. Sambrook, J., Fritsch, E. F., and Maniatis, T. (1989) *Molecular Cloning: A Laboratory Manual*, 2nd Ed., Cold Spring Harbor Laboratory, Cold Spring Harbor, NY
28. Eaton, R. W., and Chapman, P. J. (1995) *J. Bacteriol.* **177,** 6983–6988
29. Luu, P. P., Yung, C. W., Sun, A. K.-Y., and Wood, T. K. (1995) *Appl. Microbiol. Biotechnol.* **44,** 259–264
30. Sanger, F., Nicklen, S., and Coulson, A. R. (1977) *Proc. Natl. Acad. Sci. U. S. A.* **74,** 5463–5467
31. Morris, G. M., Goodsell, D. S., Halliday, R. S., Huey, R., Hart, W. E., Belew, R. K., and Olson, A. J. (1998) *J. Comput. Chem.* **19,** 1639–1662
32. Goodsell, D. S., and Olson, A. J. (1990) *Proteins* **8,** 195–202
33. Guex, N., and Peitsch, M. C. (1997) *Electrophoresis* **18,** 2714–2723
34. Schwede, T., Kopp, J., Guex, N., and Peitsch, M. C. (2003) *Nucleic Acids Res.* **31,** 3381–3385
35. Peitsch, M. C. (1995) *Bio/Technology* **13,** 658–660
36. Sakamoto, T., Joern, J. M., Arisawa, A., and Arnold, F. H. (2001) *Appl. Environ. Microbiol.* **67,** 3882–3887
37. Bylina, E. J., Coleman, W. J., Dilworth, M. R., Robles, S. J., Tanner, M. A., Yang, M. M., and Youvan, D. C. (2000) *ASM News* **66,** 211–217
38. Bertoni, G., Martino, M., Galli, E., and Barbieri, P. (1998) *Appl. Environ. Microbiol.* **64,** 3626–3632
39. Shim, H., Ryoo, D., Barbieri, P., and Wood, T. K. (2001) *Appl. Microbiol. Biotechnol.* **56,** 265–269
40. Smith, C. A., O'Reilly, K. T., and Hyman, M. R. (2003) *Appl. Environ. Microbiol.* **69,** 7385–7394
41. Mitchell, K. H., Rogge, C. E., Gierahn, T., and Fox, B. G. (2003) *Proc. Natl. Acad. Sci. U. S. A.* **100,** 3784–3789
42. Byrne, A. M., and Olsen, R. H. (1996) *J. Bacteriol.* **178,** 6327–6337
43. Kahng, H.-Y., Byrne, A. M., Olsen, R. H., and Kukor, J. J. (2000) *J. Bacteriol.* **182,** 1232–1242
44. Fishman, A., Tao, Y., and Wood, T. K. (2004) *Biocatal Biotransformation*, in press
45. Branden, C., and Tooze, J. (1999) *Introduction to Protein Structure*, 2nd Ed., pp. 14–18, Garland Publishing Inc., New York
46. Rosenzweig, A. C., Brandstetter, H., Whittington, D. A., Nordlund, P., Lippard, S. J., and Frederick, C. A. (1997) *Proteins Struct. Funct. Genet.* **29,** 141–152
47. Perry, R. H., and Chilton, C. H. (1973) *Chemical Engineers' Handbook*, 5th Ed., pp. 3–39, McGraw-Hill Inc., New York
48. Zhou, N. Y., Jenkins, A., Chan Kwo Chion, C. K. N., and Leak, D. J. (1998) *FEBS Lett.* **430,** 181–185
49. Haigler, B. E., and Spain, J. C. (1991) *Appl. Environ. Microbiol.* **57,** 3156–3162
50. McMurry, J. (2004) *Organic Chemistry*, 6th Ed., pp. 528–569, Thomson Learning Inc., Belmont, CA
51. Gassner, G. T., and Lippard, S. J. (1999) *Biochemistry* **38,** 12768–12785
52. Brazeau, B. J., and Lipscomb, J. D. (2003) *Biochemistry* **42,** 5618–5631
53. Reetz, M. T., Zonta, A., Schimossek, K., Liebeton, K., and Jaeger, K. E. (1997) *Angew. Chem. Int. Ed. Engl.* **36,** 2830–2832
54. Liebeton, K., Zonta, A., Schimossek, K., Nardini, M., Lang, D., Dijkstra, B. W., Reetz, M. T., and Jaeger, K. E. (2000) *Chem. Biol.* **7,** 709–718
55. May, O., Nguyen, P. T., and Arnold, F. H. (2000) *Nat. Biotechnol.* **18,** 317–320
56. Dolfing, J., van den Wijngaard, A. J., and Janssen, D. B. (1993) *Biodegradation* **4,** 261–282
57. Jahng, D., Kim, C. S., Hanson, R. S., and Wood, T. K. (1996) *Biotechnol. Bioeng.* **51,** 349–359
58. Jahng, D., and Wood, T. K. (1994) *Appl. Environ. Microbiol.* **60,** 2473–2482